Eur. Phys. J. C (2020) 80:669
https://doi.org/10.1140/epjc/s10052-020-8240-z

THE EUROPEAN PHYSICAL JOURNAL C

Check for updates

Regular Article - Theoretical Physics

Higgs portal to dark matter and $B \to K^{(*)}$ decays

Aliaksei Kachanovich[a], **Ulrich Nierste**[b], **Ivan Nišandžić**[c]

Institute for Theoretical Particle Physics (TTP), Karlsruhe Institute of Technology (KIT), Wolfgang-Gaede-Straße 1, 76131 Karlsruhe, Germany

Received: 23 March 2020 / Accepted: 14 July 2020 / Published online: 24 July 2020
© The Author(s) 2020

Abstract We consider a Higgs portal model in which the 125-GeV Higgs boson mixes with a light singlet mediator h_2 coupling to particles of a Dark Sector and study potential $b \to s h_2$ decays in the Belle II experiment. Multiplying the gauge-dependent off-shell Standard-Model b-s-Higgs vertex with the sine of the Higgs mixing angle does not give the correct b-s-h_2 vertex. We clarify this issue by calculating the b-s-h_2 vertex in an arbitrary R_ξ gauge and demonstrate how the ξ dependence cancels from physical decay rates involving an on-shell or off-shell h_2. Then we revisit the $b \to s h_2$ phenomenology and point out that a simultaneous study of $B \to K^* h_2$ and $B \to K h_2$ helps to discriminate between the Higgs portal and alternative models of the Dark Sector. We further advocate for the use of the h_2 lifetime information contained in displaced-vertex data with h_2 decaying back to Standard-Model particles to better constrain the h_2 mass or to reveal additional h_2 decay modes into long-lived particles.

1 Introduction

The possibility of the Standard-Model (SM) Higgs field serving as the portal to dark matter [1] has been extensively phenomenologically studied in the past two decades. A viable scenario involves a gauge singlet Higgs field which mixes with the SM Higgs field through appropriate terms in the Higgs potential, resulting in a dominantly SU(2)-doublet Higgs boson h_1 with mass 125 GeV and an additional Higgs boson h_2 with a priori arbitrary mass [2–4]. If the mixing angle is sufficiently small, the couplings of the 125-GeV Higgs h_1 comply with their SM values within the experimental error bars. The other Higgs boson h_2, which is mostly gauge singlet, serves as a mediator to the Dark Sector. In the simplest models the mediator couples to pairs of dark-matter (DM) particles. In this paper we are interested in the imprints of the described Higgs portal scenario on rare B meson decays which can be studied in the new Belle II experiment. If the h_2 mass is in the desired range below the B mass, the decay of h_2 into a pair of DM particles must necessarily be kinematically forbidden to comply with the observed relic DM abundance [3,4]. Phenomenological studies of the scenario were recently performed in Refs. [4–8].

In this article we first revisit the calculation of the loop-induced amplitude $b \to s h_2$. The literature on the topic employs a result derived from the SM $\bar{s}b$-Higgs vertex with off-shell Higgs [9]. However, it is known that this vertex is gauge-dependent [10]. This observation calls for a novel calculation of the $\bar{s}bh_2$ vertex in an arbitrary R_ξ gauge in order to investigate the correctness of the standard approach and to understand how the gauge parameter ξ cancels in physical observables. After briefly reviewing the model in Sect. 2 we present our calculation of the $\bar{s}bh_2$ vertex in Sect. 3 and demonstrate the cancellation of the gauge dependence for the two cases with on-shell h_2 and an off-shell h_2 coupling to a fermion pair, respectively. In Sect. 4 we present a phenomenological analysis with several novel aspects, such as a study of the decay $B \to K^* h_2$ and a discussion of the lifetime information inferred from data on $B \to K^{(*)} h_2 [\to f\bar{f}]$ with a displaced vertex of the h_2 decay into the fermion pair $f\bar{f}$. In Sect. 5 we conclude.

2 Model

A minimal extension of the SM with a real scalar singlet boson serving as mediator to the Dark Sector involves the Higgs potential:

$$V = V_H + V_{H\phi} + V_\phi + \text{h.c.} \tag{1}$$

$$\text{with} \quad V_H = -\mu^2 H^\dagger H + \frac{\bar{\lambda}_0}{4}(H^\dagger H)^2,$$

$$V_{H\phi} = \frac{\alpha}{2}\phi(H^\dagger H),$$

[a] e-mail: aliaksei.kachanovich@kit.edu
[b] e-mail: ulrich.nierste@kit.edu
[c] e-mail: ivan.nisandzic@kit.edu (corresponding author)

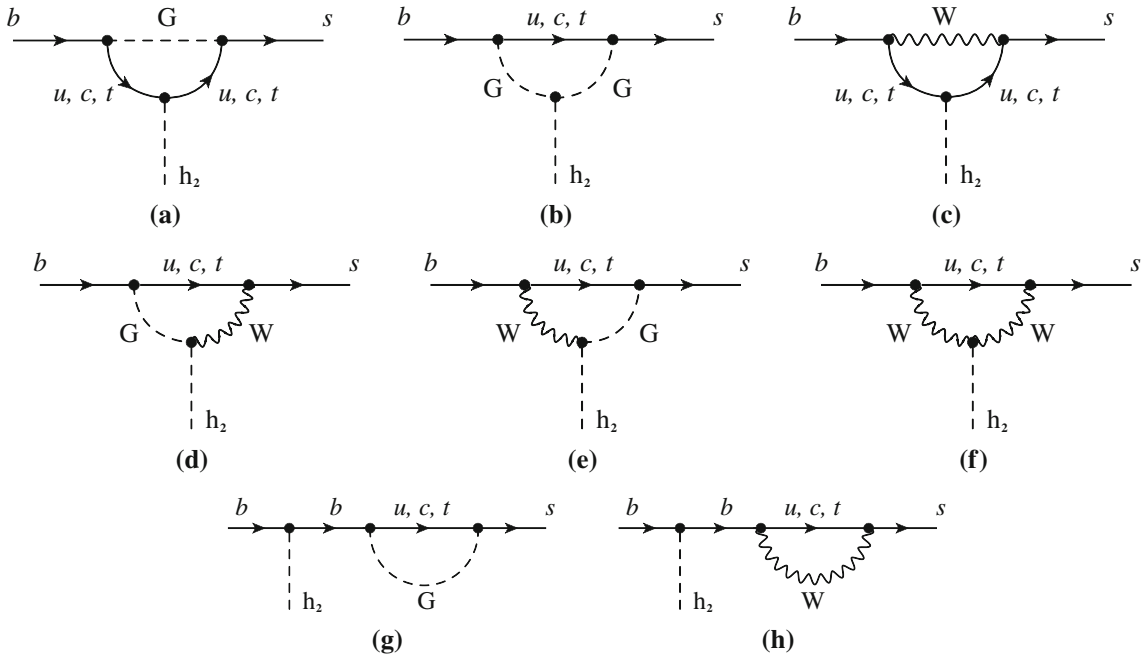

Fig. 1 One-loop diagrams contributing to $b \to s h_2$ in R_ξ gauge

$$V_\phi = \frac{m^2}{2}\phi^2 + \frac{1}{4}\lambda_\phi \phi^4,$$

where ϕ denotes the scalar singlet field in the interaction basis, while $H = \left(G^+, (v + h + iG^0)/\sqrt{2}\right)^T$ is the SM Higgs doublet. We minimize the scalar potential V with respect to ϕ and h and then choose to express the mass parameters μ and m in terms of corresponding vacuum expectation values (vevs) v_ϕ and v, respectively:

$$\begin{aligned}
\mu_h^2 &\equiv \frac{\partial^2 V}{\partial h^2} = \frac{\bar{\lambda}_0 v^2}{2}, \\
\mu_{h\phi}^2 &\equiv \frac{\partial^2 V}{\partial h \partial \phi} = \frac{\alpha v}{2}, \\
\mu_\phi^2 &\equiv \frac{\partial^2 V}{\partial \phi^2} = 2\lambda_\phi v_\phi^2 - \frac{\alpha v^2}{4 v_\phi}.
\end{aligned} \tag{2}$$

The corresponding off-diagonal mass matrix is diagonalized with the introduction of the mixing angle θ

$$h = \cos\theta\, h_1 - \sin\theta\, h_2, \quad \phi = \sin\theta\, h_1 + \cos\theta\, h_2. \tag{3}$$

As mentioned in the introduction, we choose h_2 as the light mass eigenstate, whose signatures we are primarily interested in, while h_1 corresponds to the observed Higgs boson with mass 125 GeV.

An important Feynman rule for the calculation of the scalar penguin in R_ξ gauge is the one for the $G^+G^-h_2$ vertex. After diagonalization the mass matrix we find[1]

$$\begin{aligned}
G^+G^-h_1: &\quad -i\frac{e m_{h_1}^2 \cos\theta}{2 m_W \sin\theta_W}, \\
G^+G^-h_2: &\quad i\frac{e m_{h_2}^2 \sin\theta}{2 m_W \sin\theta_W}.
\end{aligned} \tag{4}$$

One easily verifies that the rest of the vertices that are required for the studies of low energy phenomenology are simple rescalings of the corresponding SM Higgs vertices by the factor $(-\sin\theta)$. Note that the $G^+G^-h_2$ vertex is not found in the same way from the corresponding SM vertex, but in addition involves the proper replacement of the SM Higgs mass by m_{h_2}.

One could have included more terms in the scalar potential in Eq. (1) such as $\phi^2 H^\dagger H$, however, such terms would not change the low-energy phenomenology related to the process of our interest but would merely influence the scalar self-interactions that we are currently not concerned with.

3 The $\bar{s}bh_2$ vertex in the R_ξ gauge

We employ a general R_ξ gauge for the calculation of the Feynman diagrams contributing to the $\bar{s}$-b-h_2 vertex. We further use the *FeynArts* package [11] for generating the amplitudes and the *FeynCalc* [12–14], *Package-X* [15], and *FeynHelpers* [16] packages to evaluate the analytic expressions for the Feynman diagrams. Neglecting the mass of the external s quark, we encounter the diagrams shown in Fig. 1. In our final result we will also neglect the masses of the internal up and charm quarks. While the expressions for individual

[1] We express the Feynman rules using the conventions of the SM file in the *FeynArts* [11] package.

diagrams contain ultraviolet poles, the final result is UV convergent due to the Glashow–Iliopoulos–Maiani mechanism.

In order to elucidate the gauge independence of the physical quantities, we set the h_2 boson off the mass shell. In a first step we present the results in terms of the scalar loop functions B_0, C_0 of the Passarino–Veltman (PV) basis, keeping exact dependences on all momenta and masses. For the final goal to calculate the low-energy Wilson coefficient governing the decay process $b \to s\, h_2$ this appears unnecessary, but it turns out that the expression in terms of the PV basis is compact and most suitable for studying the gauge-independence of the physical quantities.

We decompose each diagram $\mathcal{A}_i$ as $\mathcal{A}_i = \tilde{\mathcal{A}}_i + \mathcal{A}_i^{(\xi)}$, with the second term $\mathcal{A}_i^{(\xi)}$ comprising all terms which depend on the W gauge parameter ξ. The expressions for $\tilde{\mathcal{A}}_i$ are collected in Appendix A. The results for the gauge-dependent pieces of the individual diagrams are rather lengthy, so we only provide the total sum

$$\sum_i \mathcal{A}_i^{(\xi)} = \sin\theta \frac{\lambda_t m_b m_t^2}{8\pi^2 v^3 (m_b^2 - p_{h_2}^2)} (p_{h_2}^2 - m_{h_2}^2) + (p_{h_2}^2 - m_b^2 + m_t^2 - m_W^2 \xi) \cdot C_0(0, m_b^2, p_{h_2}^2, m_W^2 \xi, m_t^2, m_W^2 \xi) \Big], \tag{5}$$

with $\lambda_t = V_{tb} V_{ts}^*$. Here and in the following we suppress the Dirac spinors for the b and s quarks. It follows from the expression above that the gauge-dependent contribution $\mathcal{A}^{(\xi)}$ vanishes for the case of an on-shell scalar boson, which confirms the gauge independence of the corresponding physical on-shell amplitude. We write the total $\bar{s}bh_2$ vertex $\mathcal{A} = \sum_i (\tilde{\mathcal{A}}_i + \mathcal{A}_i^{(\xi)})$ (with on-shell quarks and off-shell h_2) as

$$\mathcal{A} = G(p_{h_2}^2) + (p_{h_2}^2 - m_{h_2}^2) F(\xi, p_{h_2}^2), \tag{6}$$

with the second term equal to the expression in Eq. (5). We note that $F(\xi, p_{h_2}^2)$ does not depend on m_{h_2}. While the cancellation of ξ from $\mathcal{A}$ is obvious for an on-shell h_2, i.e. for the decay $b \to s\, h_2$, this feature is not immediately transparent for the case in which an off-shell h_2 decays into a pair of other particles. In such scenarios the gauge dependence is cancelled by other diagrams. Here we exemplify the cancellation of the gauge parameter for a model in which our mediator h_2 couples to a pair of invisible final state fermions:

$$\mathcal{L}_{\phi\chi\chi} = \lambda_\chi \phi \overline{\chi}\chi, \tag{7}$$

meaning that h_2 in $b \to s\, h_2[\to \overline{\chi}\chi]$ is necessarily off-shell [4]. In order to find the cancellation of the gauge parameter we must also consider the diagrams corresponding to $b \to s\, h_1[\to \overline{\chi}\chi]$ involving the heavy SM-like state h_1. The amplitudes involving the h_2 and h_1 propagators are proportional to $-\sin\theta$ and to $\cos\theta$, respectively:

$$\mathcal{A}_{b\text{-}s\text{-}h2} \sim -\sin\theta, \quad \mathcal{A}_{b\text{-}s\text{-}h1} \sim \cos\theta, \tag{8}$$

while the vertices $\mathcal{V}_{h_{1,2}\chi\chi}$ involving the coupling of the dark-matter fermion to the scalar bosons depend on θ as $\mathcal{V}_{h_1\chi\chi} \sim \sin\theta$ and $\mathcal{V}_{h_2\chi\chi} \sim \cos\theta$. The $b \to s\, h_{1,2}[\to \overline{\chi}\chi]$ amplitudes $\mathcal{A}_{h_{1,2}}$ can be schematically written as

$$\mathcal{A}_{h_2} = -\lambda_\chi \sin\theta\cos\theta \left(F(\xi, p^2) + \frac{G(p^2)}{p^2 - m_{h_2}^2} \right), \tag{9}$$

$$\mathcal{A}_{h_1} = \lambda_\chi \sin\theta\cos\theta \left(F(\xi, p^2) + \frac{G(p^2)}{p^2 - m_{h_1}^2} \right), \tag{10}$$

where p^2 denotes the square of the momentum transferred to the fermion pair. By adding the two amplitudes one verifies the cancellation of the gauge-dependent part $F(\xi, p^2)$. If one considers processes with off-shell $h_{1,2}$ exchange to SM fermions, such as in $b \to s\tau^+\tau^-$ with e.g. $m_{h_2} > m_b$, also box diagrams are needed for the proper gauge cancellation as found in Ref. [10] for the SM case.

We now proceed to integrate out the top quark and W boson within the gauge independent contribution $\tilde{\mathcal{A}} \equiv \sum_i \tilde{\mathcal{A}}_i$ to obtain the Wilson coefficient:

$$\mathcal{L}_{\text{eff}} = C_{h_2 sb}\, h_2\, \bar{s} P_R b + \text{h.c.}, \tag{11}$$

$$C_{h_2 sb} = -\frac{3 \sin\theta\, \lambda_t\, m_b\, m_t^2}{16\pi^2 v^3}, \tag{12}$$

where $v \simeq 246\,\text{GeV}$ is the vacuum expectation value of the Higgs doublet. This result agrees with Ref. [5], whereas it agrees with Refs. [4] and [9] up to the sign.[2]

The procedure to multiply the SM result for the $\bar{s}b$-Higgs vertex by $-\sin\theta$ to find the $\bar{s}bh_2$ vertex is not correct in an R_ξ gauge (nor for the special cases $\xi = 0$ or $\xi = 1$ of the Landau and 't Hooft–Feynman gauges) because of the subtlety with the $G^\pm$ vertices in Eq. (4). However, the missing terms are suppressed by higher powers of $m_{h_2}^2/m_W^2$ and do not contribute to the effective dimension-4 Lagrangian in Eq. (11).

4 Phenomenology

The experimental signature $B \to K\, h_2$ permits the determination of m_{h_2} from the decay kinematics, while the other relevant parameter of the model, $\sin\theta$, can be determined from the measured branching ratio $B(B \to K\, h_2)$. With increasing m_{h_2} more h_2 decay channels open and the h_2 lifetime may be in a favourable range allowing the h_2 to decay within the Belle II detector. This scenario has a characteristic

[2] The result in Ref. [4] has the sign opposite to us, while we cannot conclude which sign convention is used in Ref. [9].

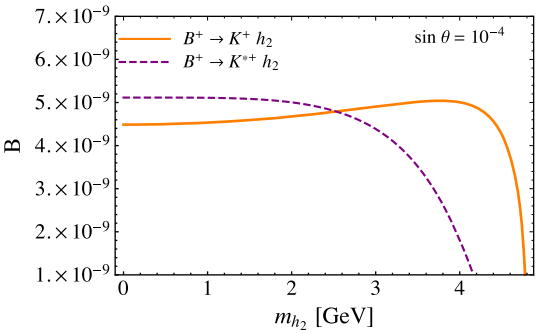

Fig. 2 Comparison of the branching fractions of $B^+ \to K^+ h_2$ (thick orange curve) and $B^+ \to K^{*+} h_2$ (dashed purple curve) for $\sin\theta = 10^{-4}$

displaced-vertex signature which is highly beneficial for the experimental analysis. Higgs-portal signatures at B factories have been widely studied [4,5,8,17–20]. In this paper we briefly revisit the recent analyses of Refs. [5,8] and complement them with novel elements: Firstly, we present a novel analysis of the decay mode $B \to K^*(892) h_2$ in comparison to $B \to K h_2$. Secondly, we highlight the benefits of the lifetime information which can be obtained from the displaced-vertex data. Thirdly, we present a new result of the number of $B \to K h_2[\to f]$ events (with f representing a pair of light particles) expected at Belle II as a function of the relevant $B \to K h_2$ and $h_2 \to f$ branching ratios.

In our study of $B \to K h_2$ and $B \to K^* h_2$ with subsequent decay of h_2 into a visible final states with displaced vertex we restrict ourselves to the case $m_{h_2} > 2m_\mu$. While the leptonic decay rate is given by the simple formula

$$\Gamma(h_2 \to \ell\ell) = \sin^2\theta \frac{G_F m_{h_2} m_\ell^2}{4\sqrt{2}\pi} \left(1 - \frac{4m_\ell^2}{m_{h_2}^2}\right)^{3/2}, \tag{13}$$

the calculation of the decay rate into an exclusive hadronic final state is challenging. Different calculations of $\Gamma(h_2 \to \pi\pi)$ and $\Gamma(h_2 \to KK)$ [21–24] employing chiral perturbation theory have been clarified, updated and refined in Ref. [5] and we use the results of this reference. In the region with $m_{h_2} > 2\,\text{GeV}$ the inclusive hadronic decay rate can be reliably calculated in perturbation theory [25].

Analyses with fully visible final states $K^{(*)} f$ can also be done at LHCb [26,27].

4.1 $B \to K h_2$

The branching ratio of $B \to K h_2$ is

$$B(B \to K h_2) = \frac{\tau_B}{32\pi m_B^2} |C_{h_2 sb}|^2 \left(\frac{m_B^2 - m_K^2}{m_b - m_s}\right)^2 \cdot f_0(m_{h_2}^2)^2 \frac{\lambda(m_B^2, m_K^2, m_{h_2}^2)^{1/2}}{2m_B}, \tag{14}$$

where $\lambda(a,b,c) = a^2 + b^2 + c^2 - 2(ab + ac + bc)$, and the scalar form factor $f_0(q^2)$ is related to the desired scalar hadronic matrix element as

$$\langle K|\bar{s}b|B\rangle = \frac{m_B^2 - m_K^2}{m_b - m_s} f_0(q^2), \tag{15}$$

where $q = p_B - p_K$. For this form factor we use the QCD lattice result of Ref. [28] (see also [29]).

The reach of the Belle II experiment for the process $B \to K h_2$ was recently studied in Ref. [8]. This investigation involves a study of the detector geometry and we present a novel study in Appendix B. For the evaluation of the number of events we use the formula Eq. (B.23). Our evaluation of the sensitivities corresponds to $5 \cdot 10^{10}$ produced $B\bar{B}$ meson pairs, where B represents both B^+ and B^0, at 50 ab^{-1} of data at Belle II experiment [30].

The parameter regions that correspond to three or more displaced vertex events of any of the final state signatures in $B \to K(h_2 \to f)$, $f = (\pi\pi + KK), \mu\mu, \tau\tau$ within the Belle II detector are displayed by the dashed red contours in Fig. 3. The number of events involve the summation over the decays of B^+, B^0 and the corresponding charge-conjugate mesons. Following Ref. [8], we display the regions in which the $\pi\pi$, KK final states occur as well as the region above the τ lepton threshold within the same plot. We show the contours of the proper lifetime of the scalar mediator within the same parameter space and encourage our experimental colleagues to include the lifetime information in the following ways: In a first step one may assume the minimal model adopted in this paper and use the lifetime measurements as additional information on m_{h_2} and $\sin\theta$. E.g. if h_2 is light enough so that the only relevant decay channel is $h_2 \to \mu^+\mu^-$, the lifetime is the inverse of the width in Eq. (13). Thanks to the strong dependence on m_{h_2} the lifetime information will improve the determination of m_{h_2} inferred from the $B \to K h_2$ decay kinematics once $\sin\theta$ is fixed from branching ratios. With more statistics one can go a step further and use the lifetime information to verify or falsify the model. Even if all h_2 couplings to SM particles originate from the SM Higgs field through mixing, a richer singlet scalar sector can change the h_2 lifetime. Consider an extra gauge singlet scalar field $\tilde{\phi}$ coupling to ϕ in the potential in Eq. (1) giving rise to a third physical Higgs state h_3. If h_3 is sufficiently light, $h_2 \to h_3 h_3$ is possible. Through $\tilde{\phi}$–H mixing the new particle h_3 will decay back into SM particles, but the lifetime can be so large that $h_2 \to h_3 h_3$ is just a missing-energy signature. Then the only detectable effect of the extra $h_2 \to h_3 h_3$ mode is a shorter h_2 lifetime. If measured precisely enough, the lifetime will permit to determine the decay rate of $h_2 \to h_3 h_3$ and thereby the associated coupling constant. Alternatively, one may fathom a model in which h_2 decays into a pair of sterile neutrinos which decay back to SM fermions.

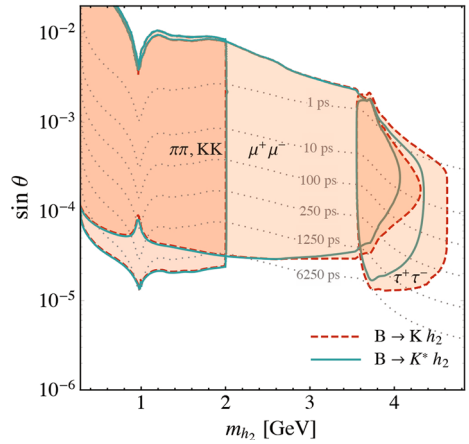

Fig. 3 Parameter regions that correspond to three or more events of $B \to K h_2 (\to f)$, $f = (\pi\pi + KK), \mu^+\mu^-, \tau^+\tau^-$ are shaded in red and bounded by the dashed red contours. Analogous regions for $B \to K^* h_2$ are presented by the dark green contour. We summed over the number of events in the decays of B^+, B^-, B^0, and $\bar{B}^0$. The dotted lines are contours of constant h_2 proper lifetime

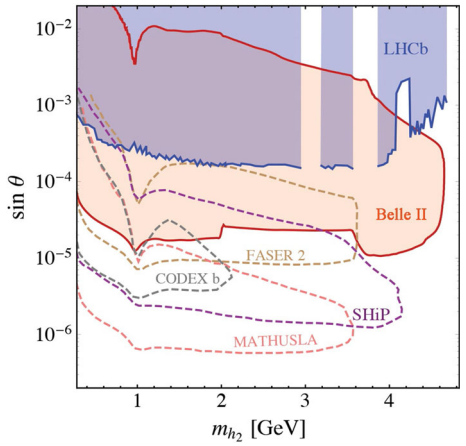

Fig. 4 Combined sensitivity of the Belle II experiment to displaced vertices of h_2 including both $B \to K h_2$ and $B \to K^* h_2$ and decays of h_2 to $(\pi\pi + KK), \mu^+\mu^-, \tau^+\tau^-$ are shown with the filled red region, and compared to the search limit of LHCb [26] (shaded blue) and projected sensitivities by other proposed experiments, Mathusla [33] (pink), SHiP [34], CODEX b [35] (gray) and FASER 2 [36] (brown)

4.2 $B \to K^* h_2$

We include in our analysis the decay of B meson that involves the final state vector meson K^* and has the branching fraction

$$B(B \to K^* h_2) = \frac{\tau_B}{32\pi m_B^2} |C_{h_2 sb}|^2 \frac{A_0(m_{h_2}^2)^2}{(m_b + m_s)^2} \cdot \frac{\lambda(m_B^2, m_{K^*}^2, m_{h_2}^2)^{3/2}}{2m_B}. \quad (16)$$

The form factor $A_0(q^2)$ is related to the desired pseudoscalar hadronic matrix element as

$$\langle K^*(k,\epsilon)|\bar{s}\gamma_5 b|B(p_B)\rangle = \frac{2\, m_{K^*}\, \epsilon^* \cdot q}{m_b + m_s} A_0(q^2), \quad (17)$$

where ϵ is a polarization vector of K^* and $q = p_B - k$. For this form factor we use the combination of results from lattice QCD [31] and QCD sum rules [32] as provided in Ref. [32].

$B(B \to K^* h_2)$ is comparable in size to $B(B \to K h_2)$ for masses up to $\sim 2\,\text{GeV}$ (see Fig. 2), and is suppressed as the mass m_{h_2} approaches the kinematic endpoint. This is the result of the additional power of the kinematic function λ in Eq. (16) that comes from the contribution of the longitudinal K^* polarization. It follows from angular momentum conservation that this is the only contributing polarization. The combination of the experimental data from both processes will be required in order to discriminate the spin-0 vs. spin-1 hypotheses in case of a discovery. E.g. the mediator with spin 1 involves a different dependence of the rate on the mediator's mass and comes with a dramatic suppression of the decay rate with K in the final state if the mediator is light. The decay $B \to K^* h_2$ has been studied before in Ref. [7], in which a plot similar to our Fig. 2 is presented for the sum of several vector resonances. Our analysis of Belle II opportunities is new compared to Ref. [7] which focuses on LHC, ShiP, and DUNE. Refs. [7,8] further study the fully inclusive decay $B \to X_s h_2$.

The kinematic suppression close to the endpoint implies that the number of $B \to K^* h_2(\tau\tau)$ events will be much smaller relative to the case of the final state with K. We display the corresponding parameter region corresponding to K^* events with the dark green contour in Fig. 3.

In Fig. 4 we compare the reach of the Belle II experiment to displaced vertices of h_2 including both $B \to K h_2$ and $B \to K^* h_2$ processes and decays of h_2 to $(\pi\pi + KK), \mu^+\mu^-, \tau^+\tau^-$ with the existing search limit of the LHCb experiment [26].[3] We also compare to projected sensitivities of other proposed experiments, Mathusla [33], SHiP [34], CODEX b [35] and FASER 2 [36].

5 Conclusions

We have clarified the cancellation of gauge-dependent terms appearing in the $\bar{s}bh_2$ vertex in the standard Higgs portal model with a singlet mediator to the Dark Sector. We have further updated the $b \to s h_2$ phenomenology to be studied at the Belle II detector, with a novel consideration of $B \to K^* h_2$ complementing the previously studied decay $B \to K h_2$. Decays like $B \to K^{(*)} h_2[\to \mu^+\mu^-]$ with a displaced vertex permit the measurement of the h_2 lifetime. It is shown how this measurement will further constrain the two relevant

[3] We use the result of Ref. [5] for the LHCb search limit on $B(B \to K h_2[\to \mu^+\mu^-])$.

parameters m_{h_2} and $\sin\theta$ of the model. Both the lifetime information and the combined study of $B \to K^* h_2$ and $B \to K h_2$ permit the discrimination of the studied Higgs portal from other Dark-Sector models. Another result of this paper is a new calculation of the expected number of $B \to K^* h_2[\to f]$ events as a function of the $B \to K h_2$ and $h_2 \to f$ branching ratios for the Belle II detector.

Acknowledgements We are grateful for helpful discussions with Teppei Kitahara, Felix Metzner, Vladyslav Shtabovenko and Susanne Westhoff and thank the authors of Ref. [8] for confirming our result in Appendix B. We further thank Ulises J. Saldaña-Salazar for participation in the early stages of the project. This work is supported by BMBF under grant *Verbundprojekt 05H2018 (ErUM-FSP T09) - BELLE II: Theoretische Studien zur Flavourphysik*. A.K. acknowledges the support from the doctoral school *KSETA* and the *Graduate School Scholarship Programme* of the *German Academic Exchange Service (DAAD)*.

Data Availability Statement This manuscript has no associated data or the data will not be deposited. [Authors' comment: The article is self-contained.]

Open Access This article is licensed under a Creative Commons Attribution 4.0 International License, which permits use, sharing, adaptation, distribution and reproduction in any medium or format, as long as you give appropriate credit to the original author(s) and the source, provide a link to the Creative Commons licence, and indicate if changes were made. The images or other third party material in this article are included in the article's Creative Commons licence, unless indicated otherwise in a credit line to the material. If material is not included in the article's Creative Commons licence and your intended use is not permitted by statutory regulation or exceeds the permitted use, you will need to obtain permission directly from the copyright holder. To view a copy of this licence, visit http://creativecommons.org/licenses/by/4.0/.
Funded by SCOAP[3].

Appendix A: Results of the loop calculation

In this appendix we present the results for the ξ-independent pieces $\tilde{\mathcal{A}}_i$ corresponding to the individual Feynman diagrams shown in Fig. 1:

$$\tilde{\mathcal{A}}_{(a)} = -\sin\theta\,\frac{\lambda_t\, m_b m_t^2}{8\pi^2 v^3}\,\frac{p_{h_2}^2 - 2m_t^2}{m_b^2 - p_{h_2}^2}\,B_0(p_{h_2}^2, m_t^2, m_t^2)$$

$$\tilde{\mathcal{A}}_{(b)} = 0, \tag{A.1}$$

$$\begin{aligned}\tilde{\mathcal{A}}_{(c)} = &-\sin\theta\,\frac{\lambda_t\, m_t^2}{16\pi^2 m_b v^3}\,\frac{1}{m_b^2 - p_{h_2}^2}\\ &\cdot\Big\{\Big[-m_b^2\big(m_W^2(4D+5x-9)+p_{h_2}^2\big)+3m_b^4\\ &+m_W^2 p_{h_2}^2(x-1)\Big]B_0(m_b^2, m_t^2, m_W^2)\\ &+2m_b^2 m_W^2\big(m_b^2(2-x)+2m_W^2(x-1)(2+x)\\ &-p_{h_2}^2\big)C_0(0, m_b^2, p_{h_2}^2, m_t^2, m_W^2, m_t^2)\\ &-4(D-2)m_b^2 m_W^2 B_0(p_{h_2}^2, m_t^2, m_t^2)\\ &+\frac{2m_W^2(m_b^2 - p_{h_2}^2)}{D-2}B_0(0, m_W^2, m_W^2)\Big\},\end{aligned} \tag{A.2}$$

$$\begin{aligned}\tilde{\mathcal{A}}_{(d)} = &-\sin\theta\,\frac{\lambda_t\, m_b}{8\pi^2 v^3}\big((m_t^2 - 2m_W^2)B_0(0, m_t^2, m_W^2)\\ &+2m_W^2 B_0(0, 0, m_W^2)\big),\end{aligned} \tag{A.3}$$

$$\begin{aligned}\tilde{\mathcal{A}}_{(e)} = &\sin\theta\,\frac{\lambda_t\, m_t^2}{16\pi^2(D-2)m_b v^3(m_b^2 - p_{h_2}^2)}\\ &\cdot\big[2m_W^2(m_b^2 - p_{h_2}^2)B_0(0, m_W^2, m_W^2)\\ &-(D-2)\big(m_b^4 - m_b^2(m_t^2 + m_W^2 + 3p_{h_2}^2)\\ &+p_{h_2}^2(m_t^2 - m_W^2)\big)B_0(m_b^2, m_t^2, m_W^2)\big],\end{aligned} \tag{A.4}$$

$$\begin{aligned}\tilde{\mathcal{A}}_{(f)} = &-\sin\theta\,\frac{\lambda_t\, m_b}{8\pi^2\, v^3(m_b^2 - p_{h_2}^2)}\Big\{m_W^2\big(2(2-D)m_W^2\\ &+2m_b^2 - m_t^2\big)B_0(m_b^2, m_t^2, m_W^2)\\ &-2m_W^2\big(m_b^2 - (D-2)m_W^2\big)B_0(m_b^2, 0, m_W^2)\\ &+m_t^2(2m_W^2 + p_{h_2}^2)B_0(p_{h_2}^2, m_W^2, m_W^2)\\ &+\big[m_t^2(2m_W^4 - m_W^2 p_{h_2}^2 + p_{h_2}^4)\\ &-4m_W^6 + 2m_b^4 m_W^2 - m_b^2\big(m_t^2(2m_W^2 + p_{h_2}^2)\\ &+2m_W^2 p_{h_2}^2\big) + m_t^4(2m_W^2 + p_{h_2}^2)\\ &+2m_W^4 p_{h_2}^2\big]C_0(0, m_b^2, p_{h_2}^2, m_W^2, m_t^2, m_W^2)\\ &-2m_W^2(-2m_W^4 + m_b^4 - m_b^2 p_{h_2}^2\\ &+m_W^2 p_{h_2}^2)C_0(0, m_b^2, p_{h_2}^2, m_W^2, 0, m_W^2)\Big\},\end{aligned} \tag{A.5}$$

$$\tilde{\mathcal{A}}_{(g)} = -\sin\theta\,\frac{\lambda_t m_t^4}{4\pi^2(D-2)m_b v^3}B_0(0, m_t^2, m_t^2), \tag{A.6}$$

$$\begin{aligned}\tilde{\mathcal{A}}_{(h)} = &\sin\theta\,\frac{\lambda_t\, m_W^2}{8\pi^2 m_b v^3}\\ &\cdot\Big[m_W^2(x-1)(D+x-2)B_0(0, m_t^2, m_W^2)\\ &+\frac{2m_t^2}{D-2}B_0(0, m_W^2, m_W^2)\\ &+(D-2)m_W^2 B_0(0, 0, m_W^2)\\ &-2m_t^2 B_0(0, m_t^2, m_t^2)\Big],\end{aligned} \tag{A.7}$$

where $\lambda_t = V_{tb}V_{ts}^*$, $x = m_t^2/m_W^2$ and $D = 4 - 2\epsilon$. The above results are to be multiplied with $\bar{s}P_R b$, where s and b denote the appropriate spinors and $P_R \equiv (1+\gamma_5)/2$.

Our definitions of Passarino–Veltman loop functions follow the *Feyncalc* package [12–14]:

$$\begin{aligned}&i\pi^2 B_0(p_1^2, m_1^2, m_2^2)\\ &= \int d^D k\,\frac{1}{(k^2 - m_1^2)\left((k+p_1)^2 - m_2^2\right)},\\ &i\pi^2 C_0(p_1^2, (p_1 - p_2)^2, p_2^2, m_1^2, m_2^2, m_3^2)\end{aligned} \tag{A.8}$$

$$= \int d^D k \frac{1}{(k^2 - m_1^2)\left((k+p_1)^2 - m_2^2\right)\left((k+p_2)^2 - m_3^2\right)}. \tag{A.9}$$

Appendix B: Evaluation of the number of events at Belle II

We describe the formula for the evaluation of the number of events in $B \to K^{(*)} h_2$, with the long-lived scalar h_2 decaying back to f, a pair of leptons or hadrons at Belle II.

The energy and the magnitude of the momentum of h_2 in the B meson rest-frame are:

$$E_{h_2} = \frac{m_B^2 + m_{h_2}^2 - m_{K^{(*)}}^2}{2m_B}, \quad |\mathbf{p}_{h_2}| = \sqrt{E_{h_2}^2 - m_{h_2}^2}. \tag{B.10}$$

For our coordinate system we choose the z-axis in the direction of the electron beam. The convention for the angle ϑ follows Chapter 3 of Ref. [30]. We consider the Lorentz transformation from the rest frame h_2 to the laboratory frame, $\mathcal{B}_1\mathcal{R}\mathcal{B}_0$, where $\mathcal{R}\mathcal{B}_0$ is the transformation from the rest frame of h_2 to the rest frame of the B meson:

$$\mathcal{R}\mathcal{B}_0 \begin{pmatrix} m_{h_2} \\ 0 \\ 0 \\ 0 \end{pmatrix} = \begin{pmatrix} E_{h_2} \\ 0 \\ |\mathbf{p}_{h_2}| \sin\vartheta_0 \\ |\mathbf{p}_{h_2}| \cos\vartheta_0 \end{pmatrix}, \tag{B.11}$$

and $\mathcal{B}_1$ is the boost from the Υ rest frame to the laboratory frame. The B meson pair is produced nearly at rest in the decay of the Υ resonance, so we neglect a small Lorentz boost from the Υ rest frame to the B rest frame. We also conveniently set the azimuthal angle ϕ to zero since it is not affected by the $\mathcal{B}_1$ boost along the z direction. The latter boost is induced by the asymmetric beam energies $E_- = 7\,\text{GeV}$ and $E_+ = 4\,\text{GeV}$ of electrons and positrons, respectively, and is determined by $\beta_B\gamma_B = (E_- - E_+)/2(E_-E_+)^{1/2} = 0.28$, $\gamma_B = 1.04$.

In the rest frame of the mediator, the decay occurs at $(c\tau, 0, 0, 0)$. The decay length in the laboratory frame follows from

$$\begin{aligned} \begin{pmatrix} ct_{\text{lab}} \\ x_{\text{lab}} \\ y_{\text{lab}} \\ z_{\text{lab}} \end{pmatrix} &= \mathcal{B}_1\mathcal{R}\mathcal{B}_0 \begin{pmatrix} c\tau \\ 0 \\ 0 \\ 0 \end{pmatrix} \\ &= \frac{c\tau}{m_{h_2}} \begin{pmatrix} \gamma_B & 0 & 0 & \gamma_B\beta_B \\ 0 & 1 & 0 & 0 \\ 0 & 0 & 1 & 0 \\ \gamma_B\beta_B & 0 & 0 & \gamma_B \end{pmatrix} \begin{pmatrix} E_{h_2} \\ 0 \\ |\mathbf{p}_{h_2}| \sin\vartheta_0 \\ |\mathbf{p}_{h_2}| \cos\vartheta_0 \end{pmatrix} \\ &= \frac{c\tau}{m_{h_2}} \begin{pmatrix} \gamma_B E_{h_2} + \gamma_B\beta_B |\mathbf{p}_{h_2}| \cos\vartheta_0 \\ 0 \\ |\mathbf{p}_{h_2}| \sin\vartheta_0 \\ \gamma_B\beta_B E_{h_2} + \gamma_B |\mathbf{p}_{h_2}| \cos\vartheta_0 \end{pmatrix}. \end{aligned} \tag{B.12}$$

The decay length of the mediator in the laboratory frame is $d_L = (x_{\text{lab}}^2 + y_{\text{lab}}^2 + z_{\text{lab}}^2)^{1/2}$ and is related to the corresponding angle ϑ as

$$y_{\text{lab}} = d_L(\vartheta_0)\sin\vartheta, \quad z_{\text{lab}} = d_L(\vartheta_0)\cos\vartheta. \tag{B.13}$$

The expected number of $B^\pm \to K^{(*)\pm} h_2[\to f]$ events is

$$\begin{aligned} N_f^\pm = N_{B^+B^-} \cdot 2 \cdot B(B^\pm \to K^{(*)\pm} h_2) B(h_2 \to f) \\ \cdot \int d\vartheta\; p(\vartheta) \frac{1}{d_L} \int_{r_{\min}(\vartheta)}^{r_{\max}(\vartheta)} dr e^{-\frac{r}{d_L}}, \end{aligned} \tag{B.14}$$

where $N_{B^+B^-}$ is the total number of produced B^+-B^- meson pairs. We include the differences in the lifetimes and the production asymmetry of B^+ and B^0 mesons:

$$\tau_{B^+} = 1.638\,\text{ps}, \qquad \tau_{B^0} = 1.519\,\text{ps}, \tag{B.15}$$

$$f^{+-} \equiv B(\Upsilon(4S) \to B^+B^-) = 0.514, \tag{B.16}$$

$$f^{00} \equiv B(\Upsilon(4S) \to B^0\bar{B}^0) = 0.486, \tag{B.17}$$

where the numerical values are taken from [37]. The total number of the displaced vertex events, summed over the decays of B^+, B^-, B^0 and $\bar{B}^0$ mesons, is

$$\begin{aligned} N_f^{\text{tot}} = N_{B\bar{B}} \cdot 2 \cdot B(B^\pm \to K^{(*)\pm} h_2) B(h_2 \to f) \\ \cdot \left(f^{+-} + f^{00}\frac{\tau_{B^0}}{\tau_{B^+}}\right) \\ \cdot \int d\vartheta\; p(\vartheta) \frac{1}{d_L} \int_{r_{\min}(\vartheta)}^{r_{\max}(\vartheta)} dr e^{-\frac{r}{d_L}}, \end{aligned} \tag{B.18}$$

where $N_{B\bar{B}} \equiv N_{B^+B^-} + N_{B^0\bar{B}^0} = 5 \cdot 10^{10}$ is the total number of produced B meson pairs with $50\,\text{ab}^{-1}$ of data at the Belle II experiment [30]. With Eq. (B.17) we find

$$\begin{aligned} N_f^{\text{tot}} = N_{B\bar{B}} \cdot 1.93 \cdot B(B^\pm \to K^{(*)\pm} h_2) B(h_2 \to f) \\ \cdot \int d\vartheta\; p(\vartheta) \frac{1}{d_L} \int_{r_{\min}(\vartheta)}^{r_{\max}(\vartheta)} dr e^{-\frac{r}{d_L}}. \end{aligned} \tag{B.19}$$

The angular distribution of the mediator in the B meson rest frame is trivial:

$$p(\vartheta_0) = \frac{1}{2}\sin\vartheta_0, \tag{B.20}$$

whereas the distribution with respect to the angle in the laboratory frame ϑ is

$$p(\vartheta) = \frac{1}{2}\sin\vartheta_0 \left|\frac{d\vartheta_0}{d\vartheta}\right|, \tag{B.21}$$

where we can express the angle ϑ_0 in terms of ϑ using Eq. (B.13).

Table 1 Total number N_f^{tot} of displaced-vertex $B \to K^{(*)} h_2[\to f]$ events (see Eq. (B.23)) occurring in the CDC of Belle II for various values of the proper lifetime (columns) and mass (rows) of h_2. All charges of the final state mesons K and K^* are included, as well as $f = \mu\mu, \tau\tau, \pi\pi, KK$

m_{h_2} (GeV)	τ (ps)				
	250	500	1000	2000	4000
0.3	50,204	18,385	5734	1614	429
0.9	972.3	465	191.8	65.7	19.6
1.5	1634.7	815.2	382.7	152.7	50.9
2.1	334.2	167.6	82.6	36.8	13.7
2.7	115.6	58	29	13.9	5.8
3.3	56.8	28.6	14.4	7.1	3.2
3.9	58.4	29.6	14.9	7.4	3.6

The maximally travelled distance in the Belle II detector as a function of the angle ϑ is given by the geometry of the compact drift chamber (CDC). Following Chapter 3 of Ref. [30] we find:

$$\begin{aligned}
\vartheta &\in \left(0.3, \arctan\frac{h}{d_1}\right), \quad r_{\max} = \frac{d_1}{\cos\vartheta}, \\
\vartheta &\in \left(\arctan\frac{h}{d_1}, \frac{\pi}{2} + \arctan\frac{d_2}{h}\right), \quad r_{\max} = \frac{h}{\sin\vartheta}, \\
\vartheta &\in \left(\frac{\pi}{2} + \arctan\frac{d_2}{h}, \frac{5\pi}{6}\right), \quad r_{\max} = -\frac{d_2}{\cos\vartheta},
\end{aligned} \tag{B.22}$$

where d_1 (d_2) is the dimension of the CDC along the positive (negative) z-direction measured from the interaction point and h is the height measured from the beam line. In our evaluation we use $d_1 = 1.5\,\text{m}$, $d_2 = 0.74\,\text{m}$, $h = 1.17\,\text{m}$.

Following Ref. [8] we use for the minimal vertex resolution $r_{\min} = 500\,\mu m$ in the formula Eq. (B.19), but neglect its dependence on ϑ. Our final formula is:

$$\begin{aligned}
N_f^{\text{tot}} = N_{B\bar{B}} \cdot 1.93 \cdot B(B^{\pm} \to K^{(*)\pm} h_2) B(h_2 \to f) \\
\cdot \int d\vartheta \, \sin\vartheta_0(\vartheta) \left|\frac{d\vartheta_0(\vartheta)}{d\vartheta}\right| \left(e^{-\frac{r_{\min}}{d_L(\vartheta)}} - e^{-\frac{r_{\max}(\vartheta)}{d_L(\vartheta)}}\right).
\end{aligned} \tag{B.23}$$

We tabulate the total number of displaced vertex events N_f^{tot} for interesting values for the proper lifetime τ and mass of h_2 in Table 1.

References

1. B. Patt, F. Wilczek, Higgs-field portal into hidden sectors. arXiv:hep-ph/0605188
2. R.M. Schabinger, J.D. Wells, A minimal spontaneously broken hidden sector and its impact on Higgs boson physics at the large hadron collider. Phys. Rev. D **72**, 093007 (2005). arXiv:hep-ph/0509209
3. A. Greljo, J. Julio, J.F. Kamenik, C. Smith, J. Zupan, Constraining Higgs mediated dark matter interactions. JHEP **1311**, 190 (2013). arXiv:1309.3561 [hep-ph]
4. G. Krnjaic, Probing light thermal dark-matter with a Higgs portal mediator. Phys. Rev. D **94**(7), 073009 (2016). arXiv:1512.04119 [hep-ph]
5. M.W. Winkler, Decay and detection of a light scalar boson mixing with the Higgs boson. Phys. Rev. D **99**(1), 015018 (2019). arXiv:1809.01876 [hep-ph]
6. S. Matsumoto, Y.L.S. Tsai, P.Y. Tseng, Light fermionic WIMP dark matter with light scalar mediator. JHEP **1907**, 050 (2019). arXiv:1811.03292 [hep-ph]
7. I. Boiarska, K. Bondarenko, A. Boyarsky, V. Gorkavenko, M. Ovchynnikov, A. Sokolenko, Phenomenology of GeV-scale scalar portal. JHEP **1911**, 162 (2019). arXiv:1904.10447 [hep-ph]
8. A. Filimonova, R. Schäfer, S. Westhoff, Probing dark sectors with long-lived particles at Belle II. Phys. Rev. D **101**(9), 095006 (2020). https://doi.org/10.1103/PhysRevD.101.095006. arXiv:1911.03490 [hep-ph]
9. B. Batell, M. Pospelov, A. Ritz, Multi-lepton signatures of a hidden sector in rare B decays. Phys. Rev. D **83**, 054005 (2011). arXiv:0911.4938 [hep-ph]
10. F.J. Botella, C.S. Lim, Flavor changing Yukawa coupling in the standard model and muon polarization in $K_L \to \mu\bar{\mu}$. Phys. Rev. Lett. **56**, 1651 (1986)
11. T. Hahn, Generating Feynman diagrams and amplitudes with FeynArts 3. Comput. Phys. Commun. **140**, 418 (2001). arXiv:hep-ph/0012260
12. R. Mertig, M. Bohm, A. Denner, FEYN CALC: computer algebraic calculation of Feynman amplitudes. Comput. Phys. Commun. **64**, 345 (1991)
13. V. Shtabovenko, R. Mertig, F. Orellana, New developments in FeynCalc 9.0. Comput. Phys. Commun. **207**, 432 (2016). arXiv:1601.01167 [hep-ph]
14. V. Shtabovenko, R. Mertig, F. Orellana, FeynCalc 9.3: new features and improvements. arXiv:2001.04407 [hep-ph]
15. H.H. Patel, Package-X: a mathematica package for the analytic calculation of one-loop integrals. Comput. Phys. Commun. **197**, 276 (2015). arXiv:1503.01469 [hep-ph]
16. V. Shtabovenko, FeynHelpers: connecting FeynCalc to FIRE and Package-X. Comput. Phys. Commun. **218**, 48 (2017). arXiv:1611.06793 [physics.comp-ph]
17. J.F. Kamenik, C. Smith, FCNC portals to the dark sector. JHEP **1203**, 090 (2012). arXiv:1111.6402 [hep-ph]
18. K. Schmidt-Hoberg, F. Staub, M.W. Winkler, Constraints on light mediators: confronting dark matter searches with B physics. Phys. Lett. B **727**, 506 (2013). arXiv:1310.6752 [hep-ph]
19. J.D. Clarke, R. Foot, R.R. Volkas, Phenomenology of a very light scalar (100 MeV$<m_h<$10 GeV) mixing with the SM Higgs. JHEP **1402**, 123 (2014). arXiv:1310.8042 [hep-ph]
20. D. Aristizabal Sierra, F. Staub, A. Vicente, Shedding light on the $b \to s$ anomalies with a dark sector. Phys. Rev. D **92**(1), 015001 (2015). arXiv:1503.06077 [hep-ph]
21. M.B. Voloshin, Once again about the role of gluonic mechanism in interaction of light Higgs boson with hadrons. Sov. J. Nucl. Phys. **44**, 478 (1986) [Yad. Fiz. **44**, 738 (1986)]
22. T.N. Truong, R.S. Willey, Branching ratios for decays of light Higgs bosons. Phys. Rev. D **40**, 3635 (1989)
23. J.F. Donoghue, J. Gasser, H. Leutwyler, The decay of a light Higgs boson. Nucl. Phys. B **343**, 341 (1990)
24. A. Monin, A. Boyarsky, O. Ruchayskiy, Hadronic decays of a light Higgs-like scalar. Phys. Rev. D **99**(1), 015019 (2019). arXiv:1806.07759 [hep-ph]
25. B. Grinstein, L.J. Hall, L. Randall, Do B meson decays exclude a light Higgs? Phys. Lett. B **211**, 363 (1988)

26. R. Aaij et al. (LHCb Collaboration), Search for long-lived scalar particles in $B^+ \to K^+\chi(\mu^+\mu^-)$ decays. Phys. Rev. D **95**(7), 071101 (2017). arXiv:1612.07818 [hep-ex]
27. R. Aaij et al. (LHCb Collaboration), Search for hidden-sector bosons in $B^0 \to K^{*0}\mu^+\mu^-$ decays. Phys. Rev. Lett. **115**(16), 161802 (2015). arXiv:1508.04094 [hep-ex]
28. J.A. Bailey et al., $B \to Kl^+l^-$ decay form factors from three-flavor lattice QCD. Phys. Rev. D **93**(2), 025026 (2016). arXiv:1509.06235 [hep-lat]
29. C. Bouchard et al. (HPQCD Collaboration), Rare decay $B \to K\ell^+\ell^-$ form factors from lattice QCD. Phys. Rev. D **88**(5), 054509 (2013). arXiv:1306.2384 [hep-lat] [Erratum: Phys. Rev. D **88**(7), 079901 (2013)]
30. E. Kou et al. (Belle-II Collaboration), The Belle II physics book. PTEP **2019**(12), 123C01 (2019). arXiv:1808.10567 [hep-ex]
31. R.R. Horgan, Z. Liu, S. Meinel, M. Wingate, Lattice QCD calculation of form factors describing the rare decays $B \to K^*\ell^+\ell^-$ and $B_s \to \phi\ell^+\ell^-$. Phys. Rev. D **89**(9), 094501 (2014). arXiv:1310.3722 [hep-lat]
32. A. Bharucha, D.M. Straub, R. Zwicky, $B \to V\ell^+\ell^-$ in the Standard Model from light-cone sum rules. JHEP **1608**, 098 (2016). arXiv:1503.05534 [hep-ph]
33. J.A. Evans, Detecting hidden particles with MATHUSLA. Phys. Rev. D **97**(5), 055046 (2018). arXiv:1708.08503 [hep-ph]
34. S. Alekhin et al., A facility to search for hidden particles at the CERN SPS: the SHiP physics case. Rep. Prog. Phys. **79**(12), 124201 (2016). arXiv:1504.04855 [hep-ph]
35. V.V. Gligorov, S. Knapen, M. Papucci, D.J. Robinson, Searching for long-lived particles: a compact detector for exotics at LHCb. Phys. Rev. D **97**(1), 015023 (2018). arXiv:1708.09395 [hep-ph]
36. A. Ariga et al. (FASER Collaboration), FASER's physics reach for long-lived particles. Phys. Rev. D **99**(9), 095011 (2019). arXiv:1811.12522 [hep-ph]
37. Y.S. Amhis et al. (HFLAV Collaboration), Averages of b-hadron, c-hadron, and τ-lepton properties as of 2018. arXiv:1909.12524 [hep-ex]